Behaviors of microtubules depend on two critical concentrations

Erin M. Jonasson[a,1], Ava J. Mauro[b,d,2], Chunlei Li[b,3], Ellen C. Norby[a,4], Shant M. Mahserejian[b,5], Jared P. Scripture[a], Ivan V. Gregoretti[a,6], Mark S. Alber[b,7], and Holly V. Goodson[a,c]

[a]Department of Chemistry and Biochemistry; [b]Department of Applied and Computational Mathematics and Statistics; [c]Department of Biological Sciences
University of Notre Dame, Notre Dame, IN 46556;
[d]Department of Mathematics and Statistics,
University of Massachusetts Amherst, Amherst MA, 01003

Classification: Biological Sciences: Cell Biology
Keywords: microtubule, dynamic instability, critical concentration, steady-state polymer
Short Title: Two microtubule critical concentrations

Present Affiliations:
[1] Department of Natural Sciences, Saint Martin's University, Lacey, WA 98503
[2] Department of Chemistry and Biochemistry, University of Notre Dame, Notre Dame, IN 46556
[3] AML, Apple, Sunnyvale, CA 94085
[4] Department of Biochemistry, Stanford University, Stanford, CA 94305
[5] Pacific Northwest National Laboratory, Richland, WA 99352
[6] Cell Signaling Technologies, Danvers, MA 01923
[7] Department of Mathematics, University of California, Riverside, CA 92521

Author for correspondence:
Holly Goodson
Department of Chemistry and Biochemistry
251 Nieuwland Science Hall
Notre Dame, IN 46556
hgoodson@nd.edu
(574) 631-7744

ABSTRACT

The concept of critical concentration is a central idea in understanding the behaviors of microtubules (MTs) and other steady-state (energy-utilizing, non-equilibrium) cytoskeletal polymers. Classically, the critical concentration (CC) is the concentration of subunits necessary to obtain polymer. However, the classical theory used to explain and predict CC is based on equilibrium polymers and fails to account for dynamic instability (DI). It has been unclear how the classical theory should be adjusted to incorporate DI or how the behavior of an individual dynamically unstable filament relates to that of its population. To address these questions, we used previously established simulations to follow at multiple scales the behavior of systems of computationally modeled dynamic microtubules. We show that polymers such as microtubules that exhibit dynamic instability have not one but at least two critical concentrations: one above which growth phases of individual filaments can occur transiently, and another above which the population's overall polymer mass will increase persistently. We propose that whether a steady-state polymer behaves like microtubules (displays dynamic instability) or like actin (can be modeled as an equilibrium polymer) depends on how far apart these critical concentrations are. This revised framework helps to explain and unify a wide range of experimental observations.

SIGNIFICANCE STATEMENT

Traditionally, biological polymers are thought to have one "critical concentration" (CC) where polymer assembly commences. It has been unclear how this framework should be adjusted to account for dynamic instability (prolonged periods of growth and shortening with random transitions). Using computational models, we show that microtubules have two critical concentrations: a lower CC where individual dynamically unstable microtubules can grow transiently ($CC_{IndGrow}$), and an upper CC where a population of such filaments grows persistently ($CC_{PopGrow}$). Our results show that most experiments thought to measure "the CC" actually measure $CC_{PopGrow}$. "Normal" dynamic instability (where individual filaments depolymerize back to the seed) happens at subunit concentrations below what is traditionally thought to be the lower lower limit for polymer appearance.

INTRODUCTION

The concept of critical concentration (CC) is fundamental to experimental studies of biological polymers, including microtubules (MTs) and actin, because it is used to determine the amount of subunit needed to obtain polymer. In the standard framework for predicting the behavior of biological polymers, there is one critical concentration at which polymer assembly commences (e.g., (1, 2)). However, this framework fails to account for the dynamic instability (DI) behavior of microtubules. The purpose of the work presented here is to adjust the classical understanding of critical concentration to incorporate dynamic instability. We find that DI polymers like microtubules have not one critical concentration, but at least two: a lower critical concentration at which individual microtubules can grow transiently, and a higher critical concentration at which a population of microtubules will grow persistently. Most measurements of critical concentration detect the higher value, the critical concentration for persistent population growth. What might be considered "normal" dynamic instability (i.e., dynamic instability where the MTs achieve a steady-state average length) happens at [free tubulin] between these two critical concentration values.

Traditional understanding of Critical Concentration in biological polymers

Two key observations led to the standard understanding of critical concentration and were originally made in very early studies of actin. First, no significant polymer was obtained until the total concentration of monomers reached an empirically defined concentration termed the "critical concentration" (CC) (**Figure 1A**, label **Q1**), above which polymer formed (3). Second, once the concentration of total monomers (subunits) reached this CC for polymer assembly, any additional subunits beyond this CC value were converted into polymer. The end result was that after polymerization reached its steady-state value, the concentration of subunits left in solution (**Figure 1A**, label **Q2**) was approximately equivalent to the observed critical concentration for polymer assembly (3–5).

These experimental observations were given a theoretical framework by Oosawa and colleagues, who explained the behavior of actin by developing a theory for the equilibrium assembly behavior of helical polymers (5, 6). This theory was extended to tubulin by Johnson and Borisy (4). The idea that polymer assembly commences at the critical concentration is now used routinely to design and interpret experiments involving cytoskeletal polymers (e.g., (2, 7–10)), and it is a standard topic for cell biology textbooks (e.g., (1, 11)). Over time, a set of experimental measurements and definitions of critical concentration, all generally treated as equivalent, have emerged (**Table 1**).

On the surface, it seems reasonable to apply this framework to understanding polymers like microtubules: it is broadly consistent with many experimental results (12), and it is founded on fundamental concepts of biochemical equilibria (e.g., see footnotes to **Table 1**). However, in the case of microtubules and other polymers that exhibit dynamic instability (stochastic switching between phases of growth and shortening, **Figure 1C**), it has been unclear how the critical concentration definitions in **Table 1** relate to the behaviors of individual filaments and

populations. There is also a deeper problem with this traditional approach: the theoretical foundation of the framework outlined above assumes that the polymers being studied are *equilibrium* polymers, *i.e.,* the analysis assumes that the polymer system is at thermodynamic equilibrium. At equilibrium, no energy enters or leaves the system. In contrast, microtubules are said to be *steady-state* polymers because they require a consistent input of energy (in the form of a pool of GTP) to maintain polymerization. Steady-state polymers like microtubules will be (mostly) disassembled at true thermodynamic equilibrium because the nucleotides in the system will be entirely hydrolyzed.

The issue of using equilibrium polymer theory to describe the behavior of steady-state polymers has long been recognized as being potentially problematic (3, 12-13). Nevertheless, it has been unclear how the impact of nucleotide hydrolysis should be incorporated into the outline above or how dynamic instability relates to these classical definitions of critical concentration. Hill and colleagues investigated problems related to these questions in the mid-1980s. The results of their work suggest that equilibrium models are limited in their ability to predict the behavior of steady-state polymer systems. In particular, they found evidence for two distinct critical concentrations in their microtubule simulations (e.g., (14), summarized in (15)). However, the existence of two critical concentrations in DI polymers has not been incorporated into common understanding, perhaps because Hill's early pioneering work did not clarify for readers the relationship between the behaviors of individual filaments and those of their populations. Thus, the equilibrium-based models remain the primary framework in use for understanding biological polymer systems.

Empirical evidence that the problem of critical concentration deserves attention comes from the observation that experimentally reported CC values for mammalian brain tubulin range from less than 3 µM to more than 20 µM (e.g. (2, 9, 16–18)). One potential explanation is that these differences can be attributed to variation in experimental approach, buffer conditions, or tubulin quality. However, another possibility is that at least some of the variation results from inaccurately applying equilibrium theory to a steady-state polymer system that exhibits dynamic instability. Proper application of critical concentration measurements to the design and interpretation of future experiments requires consensus on the definition of critical concentration for microtubules and similar polymers.

Computer simulations as an approach to addressing these questions

To investigate the concept of critical concentration in dynamically unstable polymers, we have used two different stochastic computational models that both simulate systems of dynamic microtubules, but do so at different levels of detail (19, 20). Computational models are ideal for addressing this type of problem because the biochemistry of the reactions can be explicitly controlled. Furthermore, "experiments" can be performed quickly and easily under conditions where it is possible to simultaneously follow the behavior of the system at all relevant scales: addition/loss of individual subunits, dynamic instability of individual filaments, and any changes in polymer mass of the population of filaments. In comparison, the necessary multi-scale analysis of microtubule systems has been difficult to achieve experimentally because

experiments have thus far been limited technically to measurements at one (or at most two) of these scales at a time.

In our simulations (19, 20), the governing rules and conditions are those that would be set by the experimenter or by intrinsic properties of the biological system. More specifically, the user defines the kinetic behavior of the subunits (i.e., rates of bond formation/rupture, GTP hydrolysis), the concentration of tubulin subunits in the system, whether the system is closed (competing) or open (non-competing), and the volume. Because microtubules in cells and in many *in vitro* experiments grow from stable seeds (nucleation sites), our simulations assume that one end is fixed (as would be the case for growth from centrosomes), and that all addition and loss occurs from the free end. For simplicity, the number of stable MT seeds is usually constant, but in some simulations we explore the impact of changing the number of stable seeds. Typical experimental results (DI parameters, concentrations of free and polymerized tubulin) are emergent properties of the system of biochemical reactions, just as they would be in a physical experiment.

Summary of Conclusions

Using these systems of simulated microtubules, we show that classical interpretations of experiments such as those shown in **Figure 1** can be very misleading in terms of understanding the behavior of individual MTs. In particular, we find that dynamically unstable polymers like microtubules have not one but at least two experimentally distinguishable critical concentrations: a lower CC where growth phases of individual filaments *can* occur *transiently*, and a higher CC where growth of the population's polymer mass *will* occur *steadily* (even while individual filaments in this population potentially still exhibit dynamic instability). To distinguish these two CC values, we call them $CC_{IndGrow}$ and $CC_{PopGrow}$, respectively. One key conclusion is that most experiments intended to measure the CC actually measure $CC_{PopGrow}$. A related conclusion is that "normal" microtubule dynamic instability (where MTs grow and depolymerize back to the seed) is limited to concentrations *below* what has classically been considered "the" CC needed for polymer assembly. The improved understanding of microtubule dynamics that results from these studies helps explain a range of *in vitro* microtubule experiments and provides a more solid foundation for understanding how *in vitro* microtubule behavior relates to that observed *in vivo*. While our studies focus on microtubules, we suggest that our critical concentration definitions and interpretations will apply to any steady-state polymer and are especially significant to those that exhibit dynamic instability.

RESULTS AND DISCUSSION

Computational Models

In this work, we used both a "simplified" model of MT dynamics, in which MTs are modeled as simple linear polymers (19), and a "detailed" model, where microtubules are composed of 13 protofilaments, with individual lateral and longitudinal bonds between subunits (tubulin dimers) modeled explicitly (20) (**Figure 2A-B**). Subunit addition/loss and GTP hydrolysis (both models) and lateral bond formation/breaking (detailed model only) are stochastic events that occur according to user-defined rate constants. As noted above, the dynamic instability parameters and the concentrations of free and polymerized tubulin subunits (abbreviated as [free Tu] and [MT polymer] respectively) at steady state are emergent properties of the systems, just as they would be in physical experiments. Both simulations spontaneously undergo the full range of dynamic instability behaviors (including rescue), and they can simulate systems of dynamic microtubules (either competing, with constant [total tubulin], or non-competing, with constant [free tubulin]) for hours of simulated time (19, 20). These attributes make the simulations ideal for the goal of understanding the behavior of systems of dynamic MTs and how this behavior relates to that of individual filaments.

The parameters of the detailed model were previously tuned to approximate the behavior of MTs *in vitro* (20); the simplified model parameters used here are modified from those of (19), which were originally tuned to match *in vivo* MT behavior. These two models produce dynamic instability behavior that is quantitatively different (see **Tables S1-S2** for DI parameters observed from these simulations, and Supplementary Information for more discussion of the simulations and their input parameters). Thus, while it is expected that any specific values for critical concentration(s) extracted from these two simulations will be different, we can use these differences to help address the questions of which conclusions are general and which (if any) might be specific to certain parameter sets or polymer types.

Initial Considerations

To begin investigating the concept of critical concentration as it applies to microtubules, we first asked whether the definitions outlined in **Table 1** are *valid* when studying microtubules, and if so, whether they are *equivalent* to each other.

The easiest of the various CC definitions to consider is CC_{KD}: although the idea that $CC_{KD} = k_{off}/k_{on} = K_D$ is frequently stated, it also is well-recognized that this relationship cannot be applied in a straightforward way to populations of dynamic microtubules (1). More specifically, experimentally observed critical concentrations for systems of dynamic MTs (however measured) cannot be equated to simple $k_{off}/k_{on} = K_D$ values because the GTP and GDP forms of tubulin have significantly different k_{on} and k_{off} values and therefore significantly different K_D values. For example, the critical concentration for GMPCPP (GTP-like) tubulin has been reported to be less than 1 µM (21), while that for GDP tubulin is very high, perhaps immeasurably so (12).

Exactly how the measured CC value for a system of dynamic microtubules relates to the K_D values for GTP and GDP tubulin is not yet known. However, intuition suggests that it must lie between the respective values for GTP and GDP tubulin (12). Consistent with this idea, experimentally reported values for tubulin CC typically lie between ~3 and ~20 µM (9, 16–18). Note that while the idea that CC = k_{off}/k_{on} = K_D cannot apply in a simple way to a system of dynamic microtubules, it *does* apply to GDP tubulin (when polymerized with certain drugs) or to systems containing only non-hydrolyzable (e.g., GTP-γS) or slowly-hydrolyzable (e.g., GMPCPP) analogs because in the absence of hydrolysis tubulin assembly is an equilibrium phenomenon (8, 22).

The invalidity of the idea that CC = K_D raises questions about the other definitions of CC, given that they are all generally treated as equivalent. First we will investigate in more detail the two most familiar definitions for CC (see also **Table 1**):
(i) $CC_{PolAssem}$ = [total subunit] needed for polymers to assemble.
(ii) $CC_{SubSoln}$ = [subunits left in solution] once steady-state polymer formation has been achieved.

In **Table 1** and the discussion below, we will use the terms Q1, Q2, etc. to refer to specific experimentally measurable quantities (i.e., values obtained through experimental approaches as indicated in the figures), and the terms $CC_{PolAssem}$, $CC_{SubSoln}$, etc. to refer to theoretical values (concepts) that may or may not correspond to particular experimentally measurable quantities.

Standard experimental approaches for measuring critical concentration do not yield the results predicted from traditional understanding

As discussed above, the expectation from equilibrium polymer theory is that $CC_{PolAssem}$ = $CC_{SubSoln}$, and that the value of $CC_{PolAssem}$ = $CC_{SubSoln}$ can be experimentally measured by determining Q1 or Q2 in an experiment such as those portrayed in **Figure 1A.** In other words, the expectation is that Q1 ≈ Q2, and that these experimentally obtained values provide equivalent ways to measure "the" critical concentration for polymer assembly.

We first asked whether $CC_{PolAssem}$ and $CC_{SubSoln}$ are equivalent for microtubules by performing simulations of "closed" systems where individual MTs compete for a limited pool of tubulin subunits ([total tubulin] is constant). This situation is analogous to an experiment in a test tube in which microtubules grow from pre-formed MT seeds, and both [polymer] and [free subunit] are measured at steady state.* At first glance, the behavior of the systems of simulated microtubules seemed consistent with that expected from common understanding (**Figure 1A**): significant polymer assembly was first observed at [total tubulin] ≈ Q1, and Q1 ≈ Q2 (**Figure 3A-B**).

* Unless otherwise indicated, in this manuscript we use the term "steady state" to refer specifically to polymer mass steady state, which describes a situation where the polymer mass of a closed system of dynamic MTs (i.e., a system with constant [total tubulin]) has reached a plateau and no longer changes with time (other than small fluctuations around the steady-state value). Systems of dynamic microtubules can also have other steady states (e.g., polymer length steady state). Ambiguity about which steady state a system is in can cause confusion in designing and interpreting experiments.

However, closer examination of these data showed that it is difficult to determine exactly where Q1 and Q2 are. In particular, small but non-zero amounts of polymer exist at [total tubulin] below reasonable estimates for Q1 based on extrapolating the [polymer] data back to [polymer] = 0 (**Figure S1C-F**)**.** Consistent with this observation, when we examined the behavior of the individual MTs in these simulations, we saw MTs growing and exhibiting dynamic instability at total tubulin concentrations below Q1 (**Figure 3C-D;** compare to **Figure 3A-B**). The observation that MTs exist at [total tubulin] below "the" CC as determined by Q1 is contrary to the traditional understanding of critical concentration.

In addition, it is often assumed that the concentration of unpolymerized tubulin left in solution at steady state is independent of [total tubulin] once a threshold [total tubulin] (i.e., the CC) has been reached (e.g., (23)). However, it can be seen in **Figures 3A-B** and **S1E-F** that steady-state [free tubulin] is *not* constant with respect to [total tubulin], and instead approaches a plateau represented by Q2 ≈ $CC_{SubSoln}$. In other words, $CC_{SubSoln}$ is the plateau approached by the [subunits left in solution], not the observed value of [subunits left in solution] at any particular [total subunit].

A related issue is that depending on how the Q1 extrapolation is performed, the values of Q1 and Q2 might appear different. However, if we assume that Q2 is the concentration that [free tubulin] approaches as [total tubulin] increases, and Q1 is the horizontal intercept of a line (with slope 1) that [polymer] approaches as [total tubulin] increases, then Q1 ≈ Q2 (**Figure 3A-B**), as expected. Regardless, it is evident that polymers exhibiting dynamic instability appear at [total tubulin] below Q1 ≈ Q2 (**Figures 3**, **S1**).

The sum of these data indicates that two of the major and commonly accepted predictions of equilibrium polymer theory are invalid when applied to systems of dynamic microtubules:
• Instead of both Q1 and Q2 providing an experimental measure of the concentration of subunits needed for polymer assemble ($CC_{PolAssem}$), *neither* does, since dynamically unstable MTs can be observed at concentrations below Q1 and Q2.
• Instead of all definitions of critical concentration being equivalent, $CC_{SubSoln} \neq CC_{PolAssem}$ because MTs can be observed at concentrations lower than $CC_{SubSoln}$ as measured by Q2.

The observations thus far raise two questions: (i) If $CC_{SubSoln} \neq CC_{PolAssem}$, what (if anything) is the significance of Q2 ≈ $CC_{SubSoln}$ for microtubule behavior? (ii) Is there an *actual* $CC_{PolAssem}$, i.e., a specific concentration of total subunits at which MT polymers begin to assemble?

A critical concentration for persistent growth of MT populations ($CC_{PopGrow}$)

We investigated the significance of Q2, i.e., the asymptote approached by [free tubulin] at steady state, by using our simulations to examine the amount of polymer and the mean MT length at steady state as functions of the concentration of free tubulin. For these particular studies, we fixed [free tubulin] at the indicated values instead of allowing polymer growth to deplete the free tubulin. This set of conditions is analogous to a laboratory experiment involving MTs polymerizing from stable seeds in a constantly replenishing pool of free tubulin at

known concentration, such as might exist in a flow cell. **Figure 4** shows the results of the simulation experiments:

- At low concentrations of free tubulin, there is little if any detectable MT assembly, as one might expect (**Figures 4A-B**, **S2A-B**).
- At intermediate free tubulin concentrations, both the average MT length and the concentration of MT polymer within a population reach steady-state values that increase with free tubulin but are constant with time (**Figures 4C-D**, **S2A-B**; note that these graphs have two vertical axes). In other words, the systems reach a *polymer mass steady state.* Individual microtubules in these systems exhibit what might be called "typical" dynamic instability: they undergo periods of growth and shortening with approximately random transitions (called "catastrophe" and "rescue," see **Figure 1C**), but they eventually and repeatedly depolymerize back to the stable GTP-seed (compare **Figure 4A-B** to **Figures 4C-D** and **S2A-B**).
- At still higher free tubulin concentrations, the populations of dynamic MTs undergo a major change in behavior: they begin to *grow persistently*. More specifically, when [free tubulin] is above a threshold value, there is no steady state at which the concentration of polymerized tubulin is constant over time (i.e., there is no polymer mass steady state). Instead, the system of MTs arrives at a different type of steady state where polymer mass increases at a constant rate (**Figures 4C-D**, **S2A-B**). In other words, the system of MTs reaches a *polymer growth steady state.* Individual MTs within these populations still exhibit dynamic instability (except perhaps at very high [free tubulin]), but they exhibit *net growth* over sufficient time (compare **Figure 4A-B** to **Figures 4C-D** and **S2A-B**).
- The threshold at which this behavior change occurs (Q5) can be identified from a plot of the rate of change in the steady-state polymer mass as a function of [free tubulin] (**Figure 4C-D**). Examination of this plot indicates that at concentrations of free tubulin below Q5, the population will eventually arrive at a polymer mass steady state (i.e., the rate of change in polymer mass with time ≈ zero). In contrast, at [free tubulin] above Q5, the population will increase in mass at a constant rate that increases with the concentration of free tubulin.
- Consistent with the idea that there is a [free tubulin] at which MTs begin to exhibit net growth, Dogterom and colleagues previously predicted the existence of a critical concentration at which MTs transition from exhibiting "bounded growth" to "unbounded growth"[†] (36, 37). As discussed more below, the critical concentration as predicted by Dogterom's equation evaluated with our DI measurements (**Tables S1-S2**) matches Q5 (compare + symbols to circles in **Figure 4C-D**).
- A more experimentally tractable way to identify this threshold concentration for persistent growth of MT populations is to analyze the behavior of many individual MTs within a population according to the diffusion-drift paradigm of Borisy and colleagues (25, 26). As can

[†] Note: here a "bounded" system refers to one that has a constant steady-state polymer mass or average length; "unbounded" refers to a system where the polymer mass or average length exhibits net growth over time (36, 37). We do not use the terms bounded and unbounded in defining the CC values to avoid possible confusion with situations where a system of MTs is or is not physically bounded by a barrier. This ambiguity can be especially confusing when discussing MT behaviors *in vivo* (19).

be seen in **Figure 4E-F**, a population of MTs exhibits *zero drift* at free tubulin concentrations below Q6 but exhibits *positive drift* at [free tubulin] above Q6. As one might intuitively predict, Q5 ≈ Q6.

On the basis of these observations, we conclude that microtubule populations undergo a *persistent increase in polymer mass* at free tubulin concentrations above the value identified by Q5 ≈ Q6. As averaged over long periods of time or over many individuals, the MTs in these persistently growing populations undergo *net growth* and *positive drift,* all while still experiencing dynamic instability (except perhaps at the highest tubulin concentrations). In contrast, at [free tubulin] below Q5 ≈ Q6, MT populations will (if given sufficient time) arrive at a steady-state polymer mass at which individual MTs will have a steady-state average length and experience zero *net* drift.

Significantly, Q5 ≈ Q6 lies at approximately the value of Q1 ≈ Q2, i.e., ~2.8 µM for the simplified model, and ~11.8 µM for the detailed model. This observation means that steady-state [free tubulin] in competing systems asymptotically approaches the same [free tubulin] at which microtubules begin to exhibit *net growth* (positive drift) in non-competing systems (compare Q2 in **Figure 3A-B** to Q5 ≈ Q6 in **Figure 4C-F**). Taken together, these observations show that the experimentally derived quantity Q1 ≈ Q2 ≈ Q5 ≈ Q6 does *not* yield the critical concentration for polymer assembly ($CC_{PolAssem}$) as expected from traditional understanding. Instead, these measurements yield a different CC: the CC for persistent population growth (**$CC_{PopGrow}$**).

As noted above, Dogterom and colleagues identified a critical concentration for the transition from bounded to unbounded growth, [†] where bounded and unbounded growth are characterized by the following equation (36):

$$J_{\text{Dogterom}} = \begin{matrix}\text{rate of change} \\ \text{in average length}\end{matrix} = \begin{cases} 0 & \text{during bounded growth} \\ \dfrac{(V_g\, F_{res} - |V_s| F_{cat})}{(F_{cat} + F_{res})} > 0 & \text{during unbounded growth} \end{cases}$$

Below the [free tubulin] at which the transition occurs, the average MT length reaches a finite steady-state value where the rate of change in average length is $J_{Dogterom} = 0$ (i.e., population growth is "bounded"). Above this concentration, the average MT length increases with time at a rate of $J_{Dogterom} > 0$ (i.e., population growth is "unbounded").

To determine how the critical concentration as predicted by the $J_{Dogterom}$ equation relates to the critical concentrations discussed above, we measured the DI parameters in the simulations across a range of [free tubulin] (**Tables S1**, **S2**), input the DI data into this equation, and compared the results to those obtained from directly measuring changes in average MT length (**Figure 4C-D**). Strikingly, the rates of change in average length as calculated from the DI measurements of individual MTs using the $J_{Dogterom}$ equation are very similar to the rates calculated from the net change in average length of the population of filaments (**Figure 4C-D**, compare + symbols to circles). Notably, the $J_{Dogterom}$ equation outputs become positive at approximately the same [free tubulin] as Q5. This means that the critical concentration for

unbounded growth identified by Dogterom, et al. (36, 37) agrees with the CC measured by Q1, Q2, Q5 and Q6 seen in **Figures 3-4.**

Thus, all of the approaches to measuring critical concentration discussed thus far yield the critical concentration for persistent population growth ($CC_{PopGrow}$). This conclusion leaves us with two unresolved questions: (i) What is the significance of the remaining experimental CC measurements Q3 and Q4 (**Table 1**, **Figures 5-6**)? (ii) Is there a CC at which DI polymers appear?

A critical concentration for transient elongation (growth) of individual filaments ($CC_{elongation} = CC_{IndGrow}$)

Q3 has previously been used as a measure of the so-called "critical concentration for elongation" (CC_e) (27). According to standard models, CC_e is the free subunit concentration where the rate of subunit addition to an individual filament exactly matches the rate of subunit loss from that individual filament, meaning that individual filaments should grow at subunit concentrations above CC_e (see **Table 1** and its footnotes). Thus, it is reasonable to predict that polymer assembly will commence at CC_e, implying that $CC_e = CC_{PolAssem}$.

To determine Q3 in our simulations, we used the standard approach for MTs outlined in **Table 1** (27): we plotted the growth velocity (V_g) of individual filaments as observed during the growth phase of dynamic instability as a function of [free tubulin], and extrapolated that linear relationship back to $V_g = 0$. We obtained Q3 (and thus approximate CC_e) values of ~0.65 µM for the simplified model and ~4.2 µM for the detailed model (**Figure 5A-B**). Comparing these CC_e values to the data in **Figures 3** and **4** shows that CC_e as measured by Q3 (**Figure 5A-B**) is well below $CC_{PopGrow}$ as measured by any of the other approaches (Q1 ≈ Q2 ≈ Q5 ≈ Q6). This observation demonstrates that Q3 provides information about MT behavior not provided by the other measurements.

However, the prediction that $CC_e = CC_{PolAssem}$ fails. Contrary to traditional expectation, there is *no total or free subunit concentration at which polymer assembly commences abruptly*. Instead, the amount of polymer initially increases in a slow and nonlinear way with respect to [free tubulin], increasing more rapidly only as [free tubulin] approaches $CC_{PopGrow}$ (**Figures 3-4**, **S1-S2**). The same conclusion is reached whether examining polymer mass (**Figures 3A-B**, **S1E-F**), average MT length (**Figure S2A-D**), or maximal MT length (**Figure S2C-D**). These observations mean that microtubules do not have what might be classically described as a critical concentration for polymer appearance (the theoretical $CC_{PolAssem}$ discussed earlier).

Given this information, what is the significance of CC_e? According to the approach outlined above, CC_e is the [free tubulin] value above which the growth velocity first becomes positive. In considering this question for DI polymers, it is important to remember that CC_e, as estimated by Q_3, is determined from measurements of the growth velocity of individuals *during the growth phase* of dynamic instability. Thus, CC_e provides the minimum concentration of tubulin needed for *individual* filaments to grow *transiently* (i.e., to extend during the growth phase of dynamic instability).

In contrast, as discussed above, $CC_{PopGrow}$ is determined from population-level measurements that do not separate growth and shortening behaviors (e.g., the rate of change in average length in **Figure 4C-D** is a net rate of change over both growth and shortening phases). $CC_{PopGrow}$ provides the minimum [free tubulin] necessary for the *population* of MTs (i.e., the bulk polymer) to grow *persistently*. When [free tubulin] is above $CC_{PopGrow}$, individuals may still display DI, but over time they exhibit net growth (i.e., growth outweighs shortening; on average, the MTs continually get longer with time). When [free tubulin] is below $CC_{PopGrow}$, individuals repeatedly depolymerize back to the seed (compare length history plots above and below $CC_{PopGrow}$ in **Figure 4A-B**). Consistent with the identification of the upper CC as $CC_{PopulationGrowth}$ ($CC_{PopGrow}$), we suggest referring to CC_e as $CC_{IndividualGrowth}$ ($CC_{IndGrow}$).

In considering the significance of CC_e, it is important to recognize that Q3 provides only an approximate measure of CC_e. This is because at least two of the assumptions used to measure CC_e via Q3 (see **Table 1**, footnote ***d***) are likely to be invalid, at least for mammalian brain microtubules. First, measurement of CC_e via Q3 assumes that the velocity of growth is $V_g = k_{on\_GTP}$ [GTP-tubulin] $- k_{off\_GTP}$, which implies that the off rate is independent of [free tubulin]. However, recent *in vitro* experiments have shown that the per protofilament off rate for tubulin detaching from a growing MT does depend on the tubulin concentration (20, 28, 29). This dependence of the off rate on [free tubulin] likely results from concentration-dependent differences in tip structure (20, 28, 29). Second, work with our simulations indicates that the assumption in classical CC_e measurements that only GTP subunits are exposed at the tip is likely to be invalid: GDP tubulin subunits frequently but transiently occupy the terminal position of growing (proto)filaments in both the simplified and detailed models (19, 20, 30). These observations mean that Q3 is at best an *approximation* (perhaps a bad one) of CC_e. Similar arguments hold for why Q3 provides at best only an approximate measure of K_{D_GTP} (see **Table 1**, footnote ***d***).

Appearance of MTs on stable seeds mimics a nucleation-like process without necessarily involving one

Two experimental observations have previously led to the idea that growth of MTs from stable nucleating structures (MT seeds or centrosomes) involves a nucleation-like step: (i) the fraction of stable nucleating structures occupied by MTs at different [free tubulin] follows a sigmoidal relationship (e.g., (9, 31, 32)); (ii) detectable polymers (i.e., filaments longer than the ~200 nm diffraction limit) are rare until [free tubulin] is well above Q3 ≈ $CC_{IndGrow}$ (9, 31). Suggestions for the identity of the nucleation process have included conformational maturation or sheet closure (9, 31). Both of our simulations exhibit behavior similar to experimental observations (i) and (ii) (compare **Figure 5A-B** to **Figures 5C-D** and **S2C-D**), but neither incorporates any explicit nucleation, conformational maturation, or sheet closure processes. Therefore, it is necessary to identify additional explanations for these observations.

One possibility is that the shape of the curves in **Figures 5C-D** and **S2C-D** is simply the outcome of dynamic instability itself. When [free tubulin] is just above CC_e, the growth velocity during the growth phase is low (V_g = 0 at CC_e) and the frequency of catastrophe is high (**Tables S1-S2**). Under these conditions, individual microtubules will be both short and short-lived, and so only a small amount of polymer will accumulate. As [free tubulin] rises, MTs will experience growth phases that last longer and have faster velocity, resulting in MTs that extend further. As seen by observing the average MT length or the maximum MT length, the MT lengths rise more rapidly with increasing [free tubulin], i.e., the relationship is non-linear (**Figure S2C-D**). Correspondingly, the fraction of seeds occupied by MTs with lengths above the detection threshold (**Figure 5C-D**) would be expected to increase in a similar non-linear way and thus mimic the outcome of a nucleation step without directly involving one. Because our simplified model lacks structural detail, this explanation may be sufficient to explain the sigmoidal shape of the seed-occupancy plot in that simulation (**Figure 5C**).

In our detailed model, an additional process may contribute: we have observed that in this model, non-virgin seeds in the presence of [free tubulin] near $CC_{IndGrow}$ are frequently coated by a layer of GDP tubulin left over from the previous MT.[‡] Because incoming GTP subunits will detach from these GDP subunits faster than from the GTP subunits found at the surface of a virgin seed or a growing tip, growth from a GDP-coated seed will be more difficult than extension of an already growing tip. This process could be considered to be a type of nucleation, and might be predicted to exist in physical microtubules; to our knowledge, it has not previously been considered in explanations of why growth of MTs from stable seeds appears to involve a nucleation step.

Taking all this information together, we propose that both dynamic instability itself and coating of seeds by GDP subunits contribute to the observation of nucleation-like phenomena in experimental MT growth from seeds and centrosomes (9, 31, 32). While we cannot exclude the existence of processes such as conformational maturation or sheet closure, these considerations suggest that neither hypothetical process is necessary to explain the absence of detectable MTs on seeds at [free tubulin] near $CC_{IndGrow}$.

Assessing the behavior of the polymerizing MT systems via J(c) plots

To further extend and test the understanding outlined above, we compared the CC values as measured in the simulated experiments above to those of a different and less frequently used type of experiment, the so-called "J(c) plots", where "J" (a typical abbreviation for flux) is plotted as a function of subunit concentration (see e.g., (35)) (**Figure 6**). The construction of a J(c) plot involves assessing the rate of change in polymer mass (also described as the flux into or out of polymer) after a population of MTs at steady state is diluted into a large pool of tubulin

[‡] This layer of GDP subunits becomes "stuck" on the non-hydrolyzing GTP-seed because, in our standard parameter set (20), it is the identity of the lower subunits (the ones with the exposed nucleotide) that dictate k_{off}, consistent with MT structure (33). A GDP subunit on the seed has a low k_{off} because it is attached to a GTP subunit, but incoming GTP subunits detach rapidly from this GDP subunit. This relationship has been termed "trans-acting GTP," and is expected to exist in physical MTs (34).

at a new concentration.[§] In these plots, "the CC" is identified as the concentration at which the curve crosses J = 0, i.e., where net growth = 0. At this concentration, individual MTs undergo periods of growth and shortening, but the population-level fluxes into and out of polymer are balanced. One could consider a J(c) plot to be analogous to a CC_e plot, but with measurements performed on a population with all behaviors included, instead of on individual filaments using only growth phases. We will call the CC as measured via J(c) plots "$CC_{J(c)}$." Strikingly, the value for $CC_{J(c)}$ that we measure in our simulations (see Q4 in **Figure 6**) corresponds to $CC_{PopGrow}$ as measured by the other methods.

Thus, with the exception of Q3 (**Figures 1** and **5**), which provides an estimate of $CC_{IndGrow}$, all other experimental measurements of CC (**Figure 3**, **4**, **6**) provide a measure of the critical concentration for persistent population growth ($CC_{PopGrow}$). Only Q3 provides experimental information about the concentration of tubulin needed for individual filaments to grow transiently ($CC_{IndGrow}$).

Impact of changing the number of MT seeds

Since all of the simulations above were performed with a defined number of MT nuclei (seeds), it is important to address the question of how the behaviors described above might change if the number of MT seeds is altered. Thus, we repeated the simulations of **Figure 3A** with different numbers of stable MT seeds. Examination of the results (**Figure 7A**) shows that changing the number of MT seeds does change the shape of the curves in classical CC plots. More specifically, when the number of MT seeds is small, a relatively sharp transition is seen at $CC_{PopGrow}$ in graphs of [free tubulin] and [MT polymer]; little if any bulk polymer is observed at [total tubulin] below $CC_{PopGrow}$ (**Figure 7A**). In contrast, when the number of MT seeds is high, measurable amounts of polymer appear at concentrations well below $CC_{PopGrow}$, and [free tubulin] at steady state approaches the Q2 asymptote more gradually (**Figure 7A**, compare light curves to dark curves). Regardless, the value of the Q2 asymptote (and thus $CC_{PopGrow}$) is not affected. These observations indicate that the number of MT seeds does not impact the value of $CC_{PopGrow}$, but does affect how sharply steady-state [free tubulin] approaches $CC_{PopGrow}$ (see also (4)).

The relationship between CC values, the behavior of individual filaments, and the behavior of bulk polymer

How can the above conclusion that MTs grow transiently at [tubulin] between $CC_{IndGrow}$ and $CC_{PopGrow}$ be reconciled with classical experimental observations of MTs in which bulk polymer appears abruptly at Q1 (**Figure 1A**, e.g., (4))? As discussed above, Q1 provides a measure of $CC_{PopGrow}$, but traditionally it is expected to provide the critical concentration for polymer assembly, $CC_{PolAssem.}$ This apparent conflict can be resolved by recognizing that the fraction of

[§] J(c) plots are so called because they plot polymer flux (J) as a function of concentration (c). In the physical experiments, there was normally a delay of a few seconds after the dilution and before the data were recorded. This delay may have been necessary for technical reasons, but it also serves a purpose in allowing the stabilizing GTP cap to redistribute to its steady-state size. Analysis of our simulated J(c) experiments incorporates a similar delay.

total subunits converted to polymer will be low until the free subunit concentration nears $CC_{PopGrow}$ because the average MT filament is very short at [free tubulin] below $CC_{PopGrow}$ (**Figures 4**, **S2**); under these conditions, [free tubulin] will be approximately equal to [total tubulin] unless there are many stable seeds (**Figure 7A**). In contrast, at [total tubulin] > $CC_{PopGrow}$, all subunits in excess of $CC_{PopGrow}$ will be converted to polymer if sufficient time is allowed.[**] This will happen because the average MT filament will experience net growth until [free tubulin] falls below $CC_{PopGrow}$.

The outcome of these relationships is that in bulk polymer experiments, little if any MT polymer will be detected[††] until the total tubulin concentration is above $CC_{PopGrow}$, even though dynamic individual MT filaments can transiently exist at the lower tubulin concentrations. Thus, the experimental values Q1 and Q2 may *look like* the expected critical concentration for polymer assembly $CC_{PolAssem}$, even though they actually represent the critical concentration for persistent population growth ($CC_{PopGrow}$).

Conclusions and Significance

Based on our analysis of the behavior of our computational simulations of microtubule dynamics, we conclude that the classical understanding of the relationship between subunit concentration and assembled polymer needs significant adjustment for dynamic instability polymers. In summary, for microtubules and other polymers that exhibit DI, there is no true $CC_{PolAssem}$ as classically defined. Instead, there is a lower CC ($CC_{IndGrow}$), above which *individual* filaments can grow *transiently*, and an upper CC ($CC_{PopGrow}$), above which a *population* of filaments will grow *persistently*, even while the individual filaments in this population may still undergo dynamic instability. What might be considered "normal" dynamic instability (where individual MTs repeatedly depolymerize back to the seeds) occurs at [free tubulin] between the two critical concentrations, $CC_{IndGrow}$ (estimated by Q3) and $CC_{PopGrow}$ (measured by Q1, Q2, Q4, Q5, and Q6). For a summary of our major conclusions, see **Box 1** and **Figure 7B**.

Relationship to previous work: In considering our conclusions, it is important to recognize that Hill and Chen previously suggested two critical concentrations for microtubule assembly (14) (15). However, the idea that dynamically unstable polymers have (at least) two critical concentrations is not widely recognized, perhaps because their work left unclear how the behaviors of individual filaments and their populations relate to each other and to the critical concentrations. Another characteristic that distinguishes our conclusions from those of Hill is that the Hill work investigated CC values that correspond most closely to our Q3 (**Figure 5**) and Q4 (**Figure 6**); the relationship between critical concentrations and the remainder of the experimental values (**Figures 3**, **4**) that we discuss above remained undetermined. Also significant is the work of Dogterom and colleagues, who as discussed above previously

[**] More precisely, as indicated by the earlier discussion of **Figure 3A-B**, all subunits in excess of the steady-state [free tubulin] will be converted to polymer; the steady-state [free tubulin] is necessarily below but perhaps close to $CC_{PopGrow}$.

[††] The amount of polymer *present* depends on the kinetic rate constants of the particular system and the number of stable seeds. The amount of polymer *detected* depends on the amount of polymer actually present and on what the experimental setup can detect.

predicted that there is a critical concentration at which MTs will transition between "bounded" (steady-state polymer mass) and "unbounded" (persistently growing) regimes (36, 37). However, the question of how their critical concentration for unbounded growth relates to the classical definitions of critical concentration (**Table 1**) was left unresolved. Our results in **Figure 4C-D** show that Dogterom's critical concentration corresponds most closely to our Q5 (Q5 ≈ Q1 ≈ Q2 ≈ Q4).

Significance and biological implications: We suggest that the understanding of critical concentration as presented above will help clarify apparently contradictory results in the microtubule literature. In particular, we conclude that reported measurements of "the" critical concentration for MT polymerization vary at least in part because some experiments measure $CC_{IndGrow}$ (e.g., (9)), while others measure $CC_{PopGrow.}$ (e.g., (2)). This clarification should help in design and interpretation of experiments involving critical concentration, especially those investigating the effect of MT binding proteins (e.g. (7, 9, 38)) or drugs (e.g. (8, 39)).

More importantly, these ideas help clarify the behavior of MTs *in vivo*. MTs in many interphase cell types grow persistently (perhaps with catastrophe and rescue, but with net positive drift) until they reach the cell edge, where they undergo repeated cycles of catastrophe and rescue (26). We showed previously that this persistent growth is a predictable outcome of having enough tubulin in a confined space: if sufficient tubulin is present, the MTs grow long enough to contact the cell boundary, which causes catastrophe; this drives the [free tubulin] above its natural steady-state value, which reduces catastrophe, enhances rescue, and induces the persistent growth behavior (19). In light of the current results, we can now phrase this explanation more succinctly: persistent growth of MTs in interphase cells occurs when catastrophes induced by the cell boundary drive [free tubulin] above $CC_{PopGrow}$. In contrast, at mitosis, when the MTs are more numerous and thus shorter, [free tubulin] remains below $CC_{PopGrow}$ (see also (19)(37)).

These ideas also enable a more nuanced understanding of the effects of MT binding proteins (MTBPs). MTBPs are traditionally described as being stabilizers, destabilizers, or sequestering proteins and are quantitatively characterized by their effects on DI parameters. While these descriptors remain valid, we suggest that a greater depth of understanding could be obtained by also describing a MTBP in terms of its effect on $CC_{IndGrow}$ and $CC_{PopGrow}$. For example, a protein that "stabilizes" MTs by reducing $CC_{IndGrow}$ (e.g., by increasing the fraction of incoming subunits incorporated into the MT) might be expected to increase the fraction of nuclei with active MTs; such an activity would be expected to cause an accompanying decrease in average MT length in a closed system such as a cell. In contrast, a different MTBP that stabilizes MTs by decreasing $CC_{PopGrow}$ (e.g., by increasing rescue) should result in longer MTs that are fewer in number. The idea that two proteins both categorized as "stabilizers" could have such different effects is initially confusing, but easier to understand when viewed in the light of their different effects on $CC_{IndGrow}$ and $CC_{PopGrow}$.

Another significant conclusion is the remarkable concurrence as seen in **Figure 4C-F** between three seemingly disparate ways of measuring and analyzing MT behavior: (i) the rate of change

in [MT polymer] (**Figure 4C-D**, circles), which is a bulk property obtained by assessing the mass of the population of polymers at different points in time (e.g., across 15 minutes); (ii) the $J_{Dogterom}$ equation (**Figure 4C-D**, + symbols), which uses DI parameters extracted from individual length history plots obtained over tens of minutes; (iii) the drift coefficient, which is measured from observing individual MTs in a population of MTs for short periods of time (e.g., 4 second intervals across as little as one minute see **Figures 4E-F**, **S2E-F**). These approaches differ in attributes including physical scale, temporal scale, and experimental design. The agreement between the results of these measurements suggests that the experimentally more tractable drift coefficient approach (25, 26) captures key quantitative aspects of DI and is likely to be a useful way of assessing $CC_{PopGrow}$ in the future.

Though the studies presented here were formulated specifically for MTs, we suggest that they can be applied to any nucleated, steady-state polymers that display dynamic instability. Moreover, we propose that the key characteristic that distinguishes dynamically unstable steady-state polymers (e.g. mammalian MTs) from other polymers (e.g., mammalian actin) is as follows: for DI polymers, $CC_{IndGrow}$ and $CC_{PopGrow}$ are separable values, but for the other polymers, they are either identical (as is true for equilibrium polymers) or so close as to be nearly superimposed (e.g., mammalian actin). The kinetic origins and implications of this difference are the topic of ongoing work.

METHODS

Detailed Model: The detailed computer simulation of microtubule dynamics with parameters tuned to approximate *in vitro* dynamic instability of mammalian brain MTs was described previously (20, 30, 40). The core simulation is the same as that in (20, 40), but this version has minor modifications including the addition of a dilution function to enable production of J(c) plots such as those in **Figure 6**. Please refer to the original work (20) for detailed information on the model, its parameter set C, and how its behavior compares to that of *in vitro* dynamic instability.

Simplified Model: The simplified model of microtubule dynamics was also described previously (19), but the implementation used here was updated in several major ways as described in Supplementary Information. These changes mean that the observed DI parameters (**Table S1**) and Q values (**Figures 3-7**) are not directly comparable between this implementation and our earlier publication (19), but the general behavior of the simulation is the same.

Analysis: For all analysis procedures, please see Supplementary Information.

ACKNOWLEDGMENTS

This work was supported by NSF grants MCB-0951264 and MCB-1244593 to HVG and MSA. Portions of the work were also supported by funding from the University of Massachusetts Amherst (AJM) and by a fellowship from the Dolores Zohrab Liebmann Fund (SMM). We thank the members of the Chicago Cytoskeleton community for their insightful discussions, and for members of the Goodson laboratory for assistance in editing the manuscript.

References Cited

1. Alberts B (2008) *Molecular Biology of the Cell by Bruce Alberts Published by Garland Science 5th (fifth) edition (2007) Hardcover* (Garland Science,
2. Mirigian M, Mukherjee K, Bane SL, Sackett DL (2013) Measurement of in vitro microtubule polymerization by turbidity and fluorescence. *Methods Cell Biol* 115:215–229.
3. Oosawa F, Asakura S, Hotta K, Imai N, Ooi T (1959) G-F transformation of actin as a fibrous condensation. *Journal of Polymer Science Part A: Polymer Chemistry* 37(132):323–336.
4. Johnson KA, Borisy GG (1975) The equilibrium assembly of microtubules in vitro. *Soc Gen Physiol Ser* 30:119–141.
5. Oosawa F (1970) Size distribution of protein polymers. *J Theor Biol* 27(1):69–86.
6. OOSAWA F, KASAI M (1962) A theory of linear and helical aggregations of macromolecules. *J Mol Biol* 4:10–21.
7. Amayed P, Pantaloni D, Carlier MF (2002) The effect of stathmin phosphorylation on microtubule assembly depends on tubulin critical concentration. *J Biol Chem* 277(25):22718–22724.
8. Buey RM *et al.* (2005) Microtubule interactions with chemically diverse stabilizing agents: thermodynamics of binding to the paclitaxel site predicts cytotoxicity. *Chem Biol* 12:1269–1279.
9. Wieczorek M, Bechstedt S, Chaaban S, Brouhard GJ (2015) Microtubule-associated proteins control the kinetics of microtubule nucleation. *Nat Cell Biol* 17(7):907–916.
10. Díaz-Celis C *et al.* (2017) Bacterial Tubulins A and B Exhibit Polarized Growth, Mixed-Polarity Bundling, and Destabilization by GTP Hydrolysis. *J Bacteriol* 199(19)
11. Lodish H, Berk A, Zipursky SL, al. E (2000) *Molecular cell biology* (W.H. Freeman, New York).
12. Howard J (2001) *Mechanics of Motor Proteins and the Cytoskeleton* (Sinauer Associates,
13. Wegner A, Engel J (1975) Kinetics of the cooperative association of actin to actin filaments. *Biophys Chem* 3:215–225.
14. Hill TL, Chen Y (1984) Phase changes at the end of a microtubule with a GTP cap. *Proc Natl Acad Sci U S A* 81(18):5772–5776.
15. Hill TL (2011) *Linear Aggregation Theory in Cell Biology (Springer Series in Molecular and Cell Biology)* (Springer,
16. Verdier-Pinard P, Wang Z, Mohanakrishnan AK, Cushman M, Hamel E (2000) A steroid derivative with paclitaxel-like effects on tubulin polymerization. *Mol Pharmacol* 57(3):568–575.
17. Cytoskeleton Inc. Tubulin and Microtubule Based Assays. https://www.cytoskeleton.com/custom-services3-compound-screening-tubulin-microtubules
18. Bonfils C, Bec N, Lacroix B, Harricane MC, Larroque C (2007) Kinetic analysis of tubulin assembly in the presence of the microtubule-associated protein TOGp. *J Biol Chem* 282(8):5570–5581.
19. Gregoretti IV, Margolin G, Alber MS, Goodson HV (2006) Insights into cytoskeletal behavior from computational modeling of dynamic microtubules in a cell-like environment. *J Cell Sci* 119(Pt 22):4781–4788.

20. Margolin G *et al.* (2012) The mechanisms of microtubule catastrophe and rescue: implications from analysis of a dimer-scale computational model. *Mol Biol Cell* 23(4):642–656.
21. Hyman AA, Salser S, Drechsel DN, Unwin N, Mitchison TJ (1992) Role of GTP hydrolysis in microtubule dynamics: information from a slowly hydrolyzable analogue, GMPCPP. *Mol Biol Cell* 3(10):1155–1167.
22. Díaz JF, Menéndez M, Andreu JM (1993) Thermodynamics of ligand-induced assembly of tubulin. *Biochemistry* 32(38):10067–10077.
23. Cytoskeleton Inc. Tubulin Polymerization Assay Kit Manual. http://www.cytoskeleton.com/pdf-storage/datasheets/bk006p.pdf
24. Verde F, Dogterom M, Stelzer E, Karsenti E, Leibler S (1992) Control of microtubule dynamics and length by cyclin A- and cyclin B-dependent kinases in Xenopus egg extracts. *J Cell Biol* 118(5):1097–1108.
25. Vorobjev IA, Rodionov VI, Maly IV, Borisy GG (1999) Contribution of plus and minus end pathways to microtubule turnover. *J Cell Sci* 112 (Pt 14):2277–2289.
26. Komarova YA, Vorobjev IA, Borisy GG (2002) Life cycle of MTs: persistent growth in the cell interior, asymmetric transition frequencies and effects of the cell boundary. *J Cell Sci* 115(Pt 17):3527–3539.
27. Walker RA *et al.* (1988) Dynamic instability of individual microtubules analyzed by video light microscopy: rate constants and transition frequencies. *J Cell Biol* 107(4):1437–1448.
28. Gardner MK *et al.* (2011) Rapid microtubule self-assembly kinetics. *Cell* 146(4):582–592.
29. Coombes CE, Yamamoto A, Kenzie MR, Odde DJ, Gardner MK (2013) Evolving tip structures can explain age-dependent microtubule catastrophe. *Curr Biol* 23(14):1342–1348.
30. Li C, Li J, Goodson HV, Alber MS (2014) Microtubule dynamic instability: the role of cracks between protofilaments. *Soft Matter* 10(12):2069–2080.
31. Roostalu J, Surrey T (2017) Microtubule nucleation: beyond the template. *Nat Rev Mol Cell Biol* 18(11):702–710.
32. Mitchison T, Kirschner M (1984) Microtubule assembly nucleated by isolated centrosomes. *Nature* 312(5991):232–237.
33. Rice LM, Montabana EA, Agard DA (2008) The lattice as allosteric effector: structural studies of alphabeta- and gamma-tubulin clarify the role of GTP in microtubule assembly. *Proc Natl Acad Sci U S A* 105(14):5378–5383.
34. Piedra FA *et al.* (2016) GDP-to-GTP exchange on the microtubule end can contribute to the frequency of catastrophe. *Mol Biol Cell* 27(22):3515–3525.
35. Carlier MF, Hill TL, Chen Y (1984) Interference of GTP hydrolysis in the mechanism of microtubule assembly: an experimental study. *Proc Natl Acad Sci U S A* 81(3):771–775.
36. Dogterom, Leibler (1993) Physical aspects of the growth and regulation of microtubule structures. *Phys Rev Lett* 70(9):1347–1350.
37. Dogterom M, Maggs AC, Leibler S (1995) Diffusion and formation of microtubule asters: physical processes versus biochemical regulation. *Proc Natl Acad Sci U S A* 92(15):6683–6688.
38. Hussmann F, Drummond DR, Peet DR, Martin DS, Cross RA (2016) Alp7/TACC-Alp14/TOG generates long-lived, fast-growing MTs by an unconventional mechanism. *Sci Rep*

6:20653.

39. Verma S, Kumar N, Verma V (2016) Role of paclitaxel on critical nucleation concentration of tubulin and its effects thereof. *Biochem Biophys Res Commun* 478(3):1350–1354.
40. Duan AR *et al.* (2017) Interactions between Tau and Different Conformations of Tubulin: Implications for Tau Function and Mechanism. *J Mol Biol* 429(9):1424–1438.
41. Oosawa F, Asakura S (1975) Thermodynamics of the Polymerization of Proteins (Horecker, B., Kaplan, NO, Matmur, J., and Scheraga, HA, eds) pp. 41–55.

FIGURE LEGENDS

Figure 1: Classical understanding of polymer assembly behavior. A) As typically presented in textbooks, the critical concentration (CC) of a polymer can be measured in a competing system (i.e., one where microtubules compete for tubulin subunits) by observing either the concentration of total subunits at which polymer appears (**Q1**) or the concentration of free subunits left in solution once the amount of polymer has reached steady state (**Q2**). **B)** An alternative way to measure critical concentration is to estimate the minimal concentration of subunits necessary for polymers to grow in a non-competing system (i.e., one where [free tubulin] is constant) by measuring the growth rate of individual filaments and extrapolating back to rate = 0 (**Q3**). **C)** Dynamic instability is a behavior exhibited by microtubules and some other steady-state polymers in which individual filaments undergo phases of growth and shortening separated by approximately random transitions termed *catastrophe* and *rescue*.

Figure 2: Processes that occur in the computational models. A) In the simplified model, microtubules are approximated as simple linear filaments that can undergo three processes: subunit addition, loss, and hydrolysis. Addition and loss can occur only at the tip; hydrolysis can occur anywhere in the filament where there is a GTP subunit. **B)** In the detailed model, there are 13 protofilaments, which undergo the same processes as in the simplified model but also undergo lateral bonding and breaking. In both models, the rate constants controlling these processes are input by the user, and the MTs grow off of a user-defined set of stable non-hydrolyzable GTP-tubulin seeds. The standard dynamic instability parameters (rates of growth and shrinkage, frequencies of catastrophe and rescue) are emergent properties of the input rate constants, the concentration of [free tubulin], and other aspects of the environment such as the number of stable seeds. For more information about the models and their parameter sets, see Methods, Supplementary Information, and (19, 20).

Figure 3: Behavior of microtubules (populations and individuals) under conditions of constant total tubulin. Left panels: simplified model; right panels: detailed model; colors of data points reflect the concentrations of *total* tubulin (see color keys). **A,B**) Classic critical concentration measurements. Systems of competing MTs at total tubulin concentrations as indicated on the horizontal axis were each allowed to reach polymer mass steady state. Then the average steady-state concentrations of free (squares) and polymerized (circles) tubulin subunits were measured, abbreviated as [free Tu] and [MT polymer] respectively. Data points represent the mean +/- one standard deviation of the values obtained in three independent simulations. Classically, $CC_{PolAssem}$ is estimated from **Q1**, and $CC_{SubSoln}$ is estimated from **Q2.** The main text provides justification for the idea that CC as estimated by **Q1** ≈ **Q2** provides an estimate of $CC_{PopGrow}$, the CC for persistent population growth. **C,D)** Representative length history plots for individual MTs from the simulations used in panels **A-B**. For additional data related to these simulations (e.g., plots of [free Tubulin] and [MT polymer] as functions of time), see **Figure S1**.

Figure 4: Behavior of microtubules (individuals and populations) under conditions of constant free tubulin. Left panels: simplified model; right panels: detailed model; colors of data points

reflect the concentrations of *free* tubulin (see color keys). **A,B)** Representative length history plots for one individual MT at each indicated constant free tubulin concentration. **C,D)** Rate of change in average MT length (left axis) or in concentration of total polymerized subunits ([MT polymer], right axis) between 15 and 30 minutes (circles) for the free tubulin concentrations shown; **Q5** indicates where this rate becomes positive. This panel also shows the theoretical rate of change in average MT length (+ symbol) as calculated from the extracted DI measurements (**Tables S1-S2**) using the equation $J_{Dogterom} = (V_g F_{res} - |V_s| F_{cat})/(F_{cat} + F_{res})$ (36) (see main text for discussion). Note that at concentrations below **Q5**, populations of MTs reach a steady state where the average MT length is constant (the rate of change in average length or polymer mass is approximately zero). At free tubulin concentrations above **Q5**, populations of MTs grow at a constant average rate that depends on [free tubulin]. **E,F)** Drift coefficient of MT populations as a function of [free tubulin] (x symbol), calculated according to the method of Komarova *et al.* (26). For ease of comparison, the rate of change in average MT length (circles) from panels **C,D** is re-plotted in **E,F** respectively. Note that at [free tubulin] higher than **Q6**, microtubules exhibit positive drift, and that **Q6** ≈ **Q5**. All population data points (**C-F**) represent the mean +/- one standard deviation of the values obtained in three independent simulations. The overall conclusions of the data in this figure are that (i) MTs exhibit net growth (as averaged over time or over individuals in a population) at [free tubulin] above the value **Q5** ≈ **Q6**; (ii) **Q5** ≈ **Q6** is similar to Q1 ≈ Q2 as determined in **Figure 3.** Thus, Q1, Q2, **Q5** and **Q6** all provide measures of the same critical concentration, defined as $CC_{PopGrow}$ in the main text. For additional data related to these simulations, see **Figure S2.**

Figure 5: Growth velocity of individual MTs during the growth state as a function of [free tubulin]. Left panels: simplified model; right panels: detailed model; colors of data points reflect the concentrations of *free* tubulin (see color keys). All data points (**A-D**) represent the mean +/- one standard deviation of the values obtained in three independent simulations. **A,B)** Growth velocity (V_g) during growth phases measured using an automated DI extraction tool (see **Table S1-S2** and Supplementary Information). The linear regression (fit to the V_g data from $CC_{PopGrow}$ to the highest [free tubulin]) shows that CC as measured from these plots (**Q3**) is different from that measured by Q1 ≈ Q2 ≈ Q5 ≈ Q6. The main text provides justification for the idea that **Q3** is an estimate of $CC_{IndGrow}$, the CC for transient individual filament growth. **C,D)** Fraction of stable seeds bearing "detectable" MTs as a function of [free tubulin] at 30 minutes (circles) and at 1 hour (x symbol). Here "detectable" MTs are those with length ≥ 25 dimers = 200 nm (chosen because the Abbe diffraction limit for 540 nm light in a 1.4 NA objective is ~200 nm). Taken together, the data in panels **A-B** and **C-D** show that little polymer can be detected growing off of the seeds in either simulation until [free tubulin] is well above CC_e as measured by **Q3**. Note that the lowest value of [free tubulin] at which 100 percent of the seeds have a MT of at least 200 nm corresponds to ~$CC_{PopGrow}$.

Figure 6: Flux of subunits into and out of polymerized form as a function of dilution [free tubulin] (i.e., a J(c) plot as in (35)). **A)** Simplified model and **B)** Detailed model. In these simulation experiments, competing systems of MTs at high [total tubulin] (22 μM) were allowed to polymerize until they reached polymer mass steady state, and were then shifted into ("diluted" into) the free tubulin concentrations shown on the horizontal axis; after a 5 second

delay, the flux was measured over a 10 second period, similar to (35). These data show that CC as determined from J(c) plots (**Q4**) is approximately the same value as Q1 ≈ Q2 ≈ Q5 ≈ Q6 and thus also provides a measure of $CC_{PopGrow}$. Data points for different concentrations of dilution [free tubulin] (see color key) represent the mean +/- one standard deviation of the values obtained in three independent simulations.

Figure 7: A) Impact of changing the number of microtubule seeds. Simplified model with MTs growing from 50 vs. 500 stable nuclei as shown (competing system as in **Figure 3A**; other parameters are the same). These data show that changing the number of stable MT seeds alters the approach to $CC_{PopGrow}$ (as determined by the **Q1** ≈ **Q2** values replotted here from **Figure 3A**) but does not change the value of $CC_{PopGrow}$ (compare light curves with 50 seeds to dark curves with 500 seeds). **B) Summary of the relationships between DI behavior and critical concentrations for DI polymers.** The cartoon shows [polymer] (green lines) and [free subunit] (blue lines) as would be obtained from experiments with competing systems (fixed [total subunit], similar to **Figures 3A-B** and **7A**); the text underneath the plot relates the dynamic instability behavior of individual filaments in non-competing systems (constant [free subunit], **Figure 4**) to the plot for competing systems. See **Box 1** for more explanation.

Table 1: Critical concentration definitions used in the literature. These experimental definitions have generally been treated as interchangeable; for clarity we have assigned a specific name and abbreviation to each CC as determined by a particular method. All definitions except CC_{KD} can be applied to both equilibrium and steady-state polymers. For each, we provide an example of an early publication where that definition was used.

Classical Critical Concentration definition	Abbreviation	Experimental measurement of CC as applied to MT systems
Critical concentration is the minimal concentration of total subunits (e.g., tubulin dimers) necessary for polymer assembly (4,5).	$CC_{PolAssem}$	$CC_{PolAssem}$ is determined by measuring [MT polymer][a] observed at different [total tubulin] and extrapolating back to [MT polymer] = 0. See **Q1** in **Figure 1A**; also **Figure 3A-B.**
Critical concentration is the concentration of free subunits left in solution once equilibrium or steady-state assembly[b] has been achieved (4,5).	$CC_{SubSoln}$	$CC_{SubSoln}$ is determined by measuring [free tubulin] left in solution at steady-state for different [total tubulin], and determining the position of the horizontal asymptote approached by [free tubulin]. See **Q2** in **Figure 1A**; also **Figure 3A-B.**
Critical concentration is the dissociation equilibrium constant for the binding of subunit to polymer, i.e., $CC = K_D = k_{off}/k_{on}$ [c] (41).	CC_{KD}	CC_{KD} is determined by separate experimental measurements of k_{on} and k_{off} for addition/loss of tubulin subunits to/from MT polymer and calculating the ratio k_{off}/k_{on}.
Critical concentration is the minimal concentration of free subunit required to elongate from an existing polymer[d] (27).	CC_e	CC_e is determined by measuring the growth rate during the growth state (V_{growth}) as a function of [free tubulin] and extrapolating back to $V_{growth} = 0$. See **Q3** in **Figure 1B**; also **Figure 5A-B.**
Critical concentration is the concentration of free subunit at which the flux into and out of polymer is balanced (e.g., (35)).	$CC_{J(c)}$	$CC_{J(c)}$ is determined by growing MTs to steady-state at high [total tubulin], then rapidly diluting to a new [free tubulin] and measuring the initial rate of change in [MT polymer] (i.e., [MT polymer] flux). $CC_{J(c)}$ is the value of [free tubulin] where [MT polymer] flux = 0. See **Q4** in **Figure 6.**

[a] By [MT polymer], we mean concentration of subunits in polymerized form.

[b] Assuming that assembly starts from a state with no polymer, maximal polymer assembly will occur at equilibrium for equilibrium polymers, and at polymer mass steady state for steady-state polymers.

[c] The idea that $CC = K_D$ for simple equilibrium polymers is derived straightforwardly. Briefly, the net rate of polymer length change at a single filament tip = rate of addition – rate of loss. The rate of addition is assumed to be k_{on}[free subunit], and the rate of loss is assumed to be k_{off}. Therefore, the rate at which new subunits add to a population of n polymers is $n*k_{on}$[free subunit], and the rate at which subunits detach from a population of n polymers is $n*k_{off}$. At equilibrium, rate of polymerization = rate of depolymerization, so $n*k_{on}$[free subunit] = $n*k_{off}$. Therefore, at equilibrium, [free subunit] = $k_{off}/k_{on} = K_D = CC$.

[d] The derivation justifying this CC_e definition is similar to that for CC_{KD}, but considers the behavior of a single filament, not a population, and can apply to steady-state polymers because it does not require equilibrium. For filaments like MTs that display dynamic instability, CC_e has typically been determined only from measurements taken during growth phases. Assuming that the rate of subunit addition to a single filament is k_{on}[free subunit], and that the rate of loss from that filament is k_{off}, then the overall rate of length change $V_{growth} = k_{on}$[free subunit] - k_{off}. When $V_{growth} = 0$ (i.e., the filament is neither elongating nor shortening), then [free subunit] = $k_{off}/k_{on} = CC_e$. Therefore, at [free subunit] above CC_e, the rate of subunit addition will exceed the rate of subunit loss and the polymer will grow. If one additionally assumes that a system with equal rates of addition and loss is at equilibrium, then $k_{off}/k_{on} = K_D$, and $CC_e = CC_{KD}$. In cases where the GTP and GDP forms of tubulin have different kinetic rate constants, then $k_{on\_GTP} \neq k_{on\_GDP}$ and $k_{off\_GTP} \neq k_{off\_GDP}$. Given the assumptions above, if one also assumes that growing filaments have only GTP ends, then the equation changes to $V_{growth} = k_{on\_GTP}$[free subunit] – k_{off_GTP}. When $V_{growth} = 0$, [free subunit] = $k_{off\_GTP}/k_{on\_GTP} = CC_e = K_{D\_GTP}$. Under these assumptions, both CC_e and K_{D_GTP} would be determined by Q3 (**Figure 1B**). However, it is important to recognize that because at least two of the assumptions used are questionable (see main text), Q3 provides at best an approximation of either CC_e or K_{D_GTP}. For example, for the simplified model parameter set used here, $K_{D\_GTP} = 0$ μM, but the measured Q3 value is 0.65 μM.

Box 1: The relationship between critical concentration and dynamic instability

1. Instead of one "critical concentration" for polymer assembly, microtubules have at least two critical concentrations, each with unique implications for polymer behavior (table and figure below). One is the critical concentration for transient growth of individual filaments ($CC_{IndGrow}$). The other is the critical concentration for persistent growth in the mass of a population of filaments ($CC_{PopGrow}$).

[Free Tubulin] between $CC_{IndGrow}$ and $CC_{PopGrow}$	**[Free Tubulin] above $CC_{PopGrow}$**	**Schematic Individual MT Length Histories**
The population's polymer mass grows until it arrives at a steady state where it is constant with time (i.e., it is "bounded")(24).	The population's polymer mass grows persistently (i.e., it is "unbounded")(24).	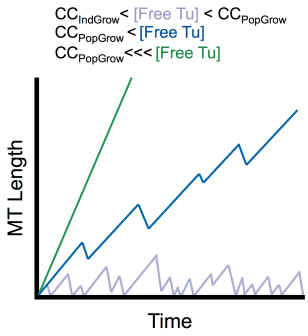
Individual filaments display dynamic instability in which they repeatedly depolymerize back to the seed (purple).	Individual filaments display dynamic instability (blue), except perhaps at very high concentrations (green), but undergo net growth over time.	
As averaged over time or many individuals, filaments exhibit zero drift (26).	As averaged over time or many individuals, filaments exhibit positive drift (26).	

2. The standard population-based experimental methods for measuring critical concentration (Q1, Q2, and Q4; see Table 1) all yield the critical concentration for persistent population growth ($CC_{PopGrow}$) (**Figures 3**, **4**, **6**). Of the standard experimental measurements, only Q3 (based on analysis of individual filaments) yields an approximation (perhaps poor) of $CC_{IndGrow}$ (**Figure 5**).
   - What might be considered "typical" steady-state dynamic instability (where filaments eventually depolymerize back to the seed) occurs at free subunit concentrations below the value Q1 ≈ Q2 ≈ Q4 ≈ Q5 ≈ Q6, which is classically considered to be "the" CC for polymer assembly (**Figure 4**).

3. The appearance of polymers on stable seeds is smooth and non-linear with respect to [free tubulin]. Filaments may not be detectable until [free tubulin] is well above $CC_{IndGrow}$ because the dependence of the DI parameters on [free tubulin] dictates a non-linear relationship between MT length and [free tubulin] (**Figure S2C-D**), mimicking a nucleation step without necessarily involving one (**Figure 5C-D**).

4. In a closed system (where filaments compete for a limited pool of subunits), [free tubulin] that is initially above $CC_{PopGrow}$ will fall to a steady-state value that is *below* but perhaps very close to $CC_{PopGrow}$ (**Figures 3A-B**, **7A**).
   - For such closed systems, a key conclusion is that steady-state [free tubulin] is not a constant independent of [total tubulin] as expected from traditional understanding of critical concentration, but is a variable that depends on [total tubulin] and on multiple other aspects of the system, such as the presence/absence of stable seeds (**Figure 7A**, see also (4)(19)).
   - Changes to the number of stable seeds will affect neither $CC_{IndGrow}$ nor $CC_{PopGrow}$, but can affect both the amount of MT polymer and the separation between steady-state [free tubulin] and $CC_{PopGrow}$ (**Figure 7A**).

Figure 1

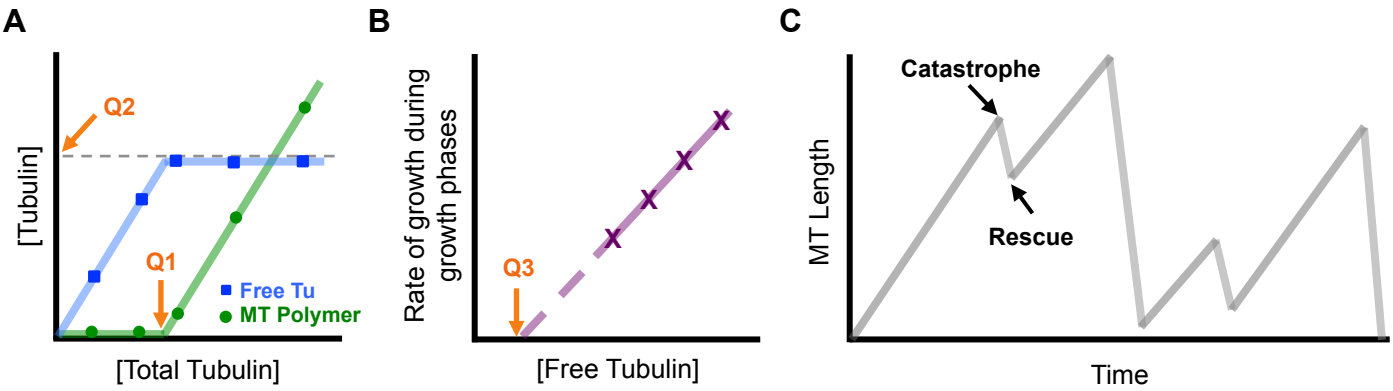
A
[Tubulin]
Q2
Q1
Free Tu
MT Polymer
[Total Tubulin]
B
Rate of growth during growth phases
Q3
[Free Tubulin]
C
MT Length
Catastrophe
Rescue
Time

Figure 2

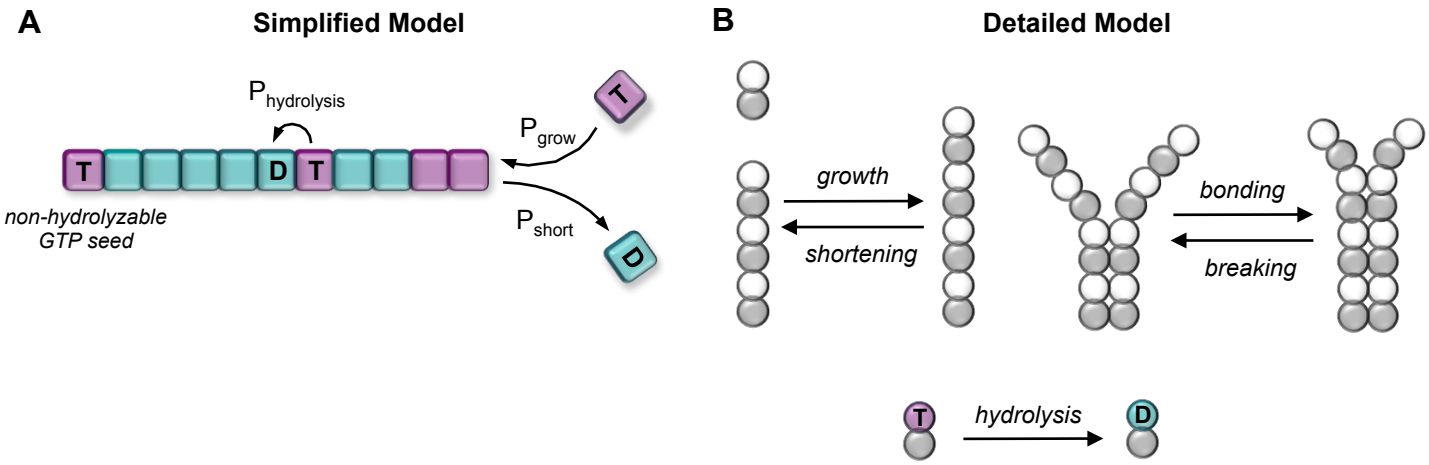
A
Simplified Model
P hydrolysis
P grow
P short
T
D
T
T
D
non-hydrolyzable
GTP seed
B
Detailed Model
growth
shortening
bonding
breaking
T
hydrolysis
D

Figure 3

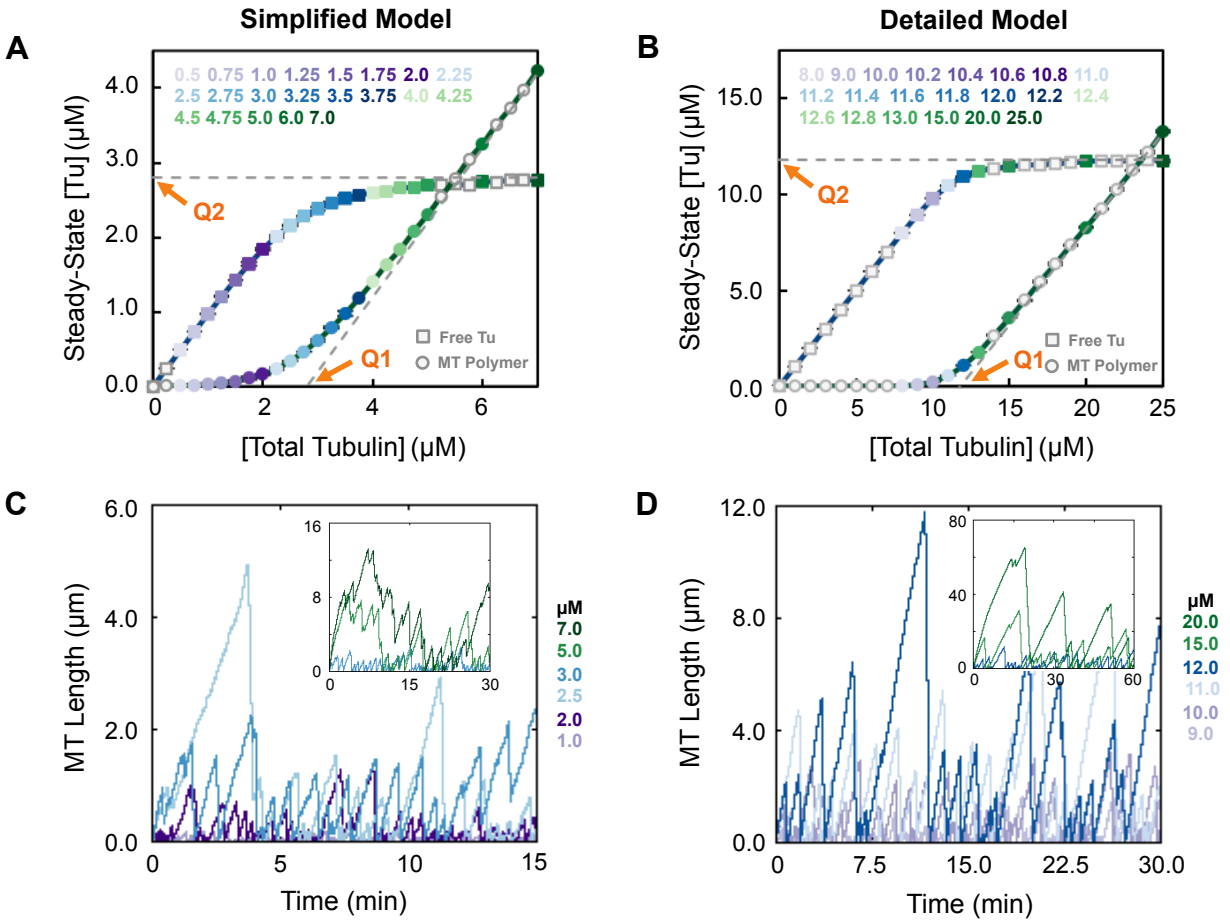
A
Simplified Model
0.5 0.75 1.0 1.25 1.5 1.75 2.0 2.25
2.5 2.75 3.0 3.25 3.5 3.75 4.0 4.25
4.5 4.75 5.0 6.0 7.0
Q2
Q1
Free Tu
MT Polymer
Steady-State [Tu] (μM)
[Total Tubulin] (μM)
B
Detailed Model
8.0 9.0 10.0 10.2 10.4 10.6 10.8 11.0
11.2 11.4 11.6 11.8 12.0 12.2 12.4
12.6 12.8 13.0 15.0 20.0 25.0
Q2
Q1
Free Tu
MT Polymer
Steady-State [Tu] (μM)
[Total Tubulin] (μM)
C
MT Length (μm)
Time (min)
μM
7.0
5.0
3.0
2.5
2.0
1.0
D
MT Length (μm)
Time (min)
μM
20.0
15.0
12.0
11.0
10.0
9.0

Figure 4

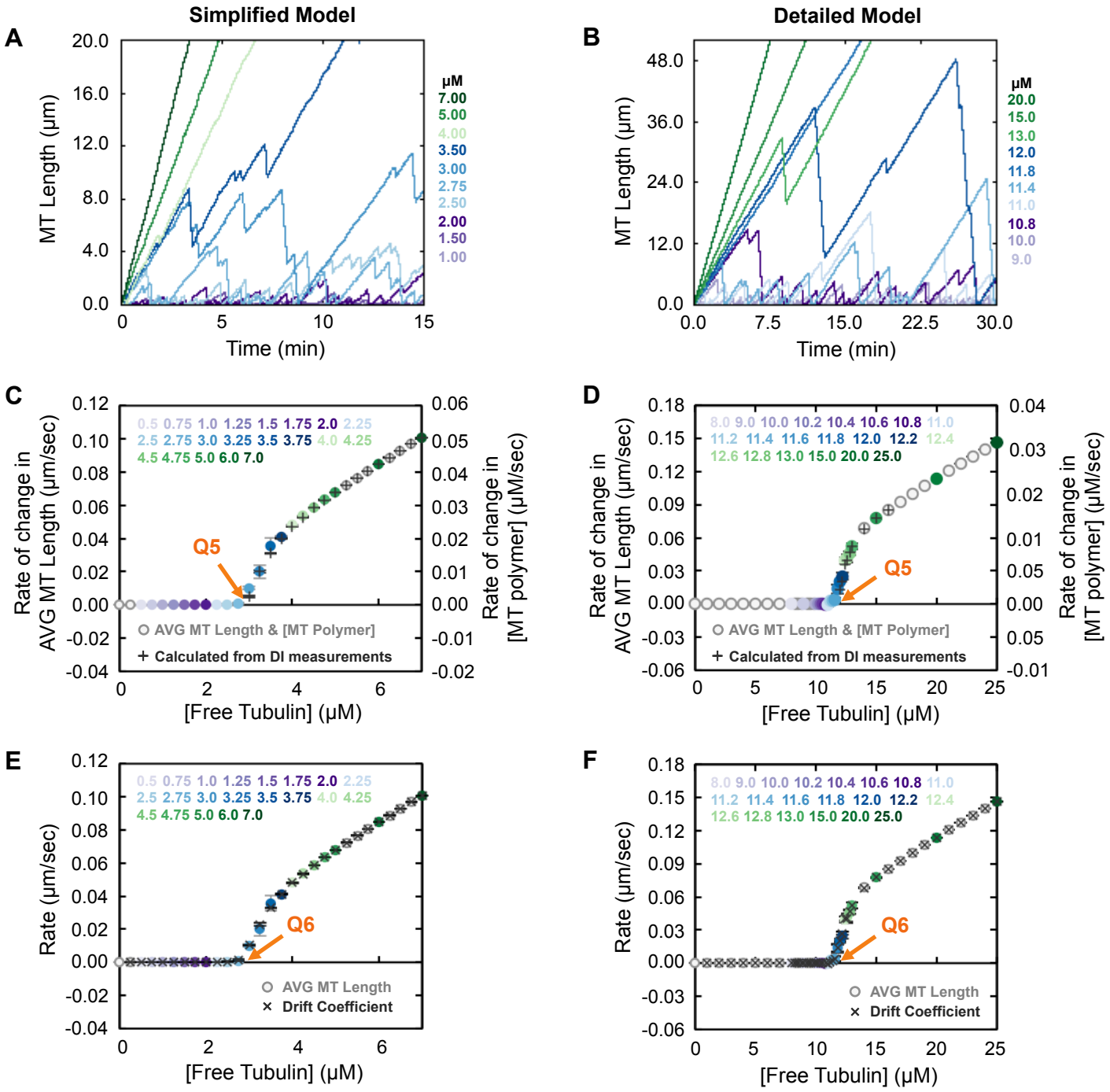
A
Simplified Model
MT Length (µm)
Time (min)
µM
7.00
5.00
4.00
3.50
3.00
2.75
2.50
2.00
1.50
1.00
B
Detailed Model
MT Length (µm)
Time (min)
µM
20.0
15.0
13.0
12.0
11.8
11.4
11.0
10.8
10.0
9.0
C
Rate of change in AVG MT Length (µm/sec)
Rate of change in [MT polymer] (µM/sec)
[Free Tubulin] (µM)
0.5 0.75 1.0 1.25 1.5 1.75 2.0 2.25
2.5 2.75 3.0 3.25 3.5 3.75 4.0 4.25
4.5 4.75 5.0 6.0 7.0
Q5
AVG MT Length & [MT Polymer]
Calculated from DI measurements
D
Rate of change in AVG MT Length (µm/sec)
Rate of change in [MT polymer] (µM/sec)
[Free Tubulin] (µM)
8.0 9.0 10.0 10.2 10.4 10.6 10.8 11.0
11.2 11.4 11.6 11.8 12.0 12.2 12.4
12.6 12.8 13.0 15.0 20.0 25.0
Q5
AVG MT Length & [MT Polymer]
Calculated from DI measurements
E
Rate (µm/sec)
[Free Tubulin] (µM)
0.5 0.75 1.0 1.25 1.5 1.75 2.0 2.25
2.5 2.75 3.0 3.25 3.5 3.75 4.0 4.25
4.5 4.75 5.0 6.0 7.0
Q6
AVG MT Length
Drift Coefficient
F
Rate (µm/sec)
[Free Tubulin] (µM)
8.0 9.0 10.0 10.2 10.4 10.6 10.8 11.0
11.2 11.4 11.6 11.8 12.0 12.2 12.4
12.6 12.8 13.0 15.0 20.0 25.0
Q6
AVG MT Length
Drift Coefficient

Figure 5

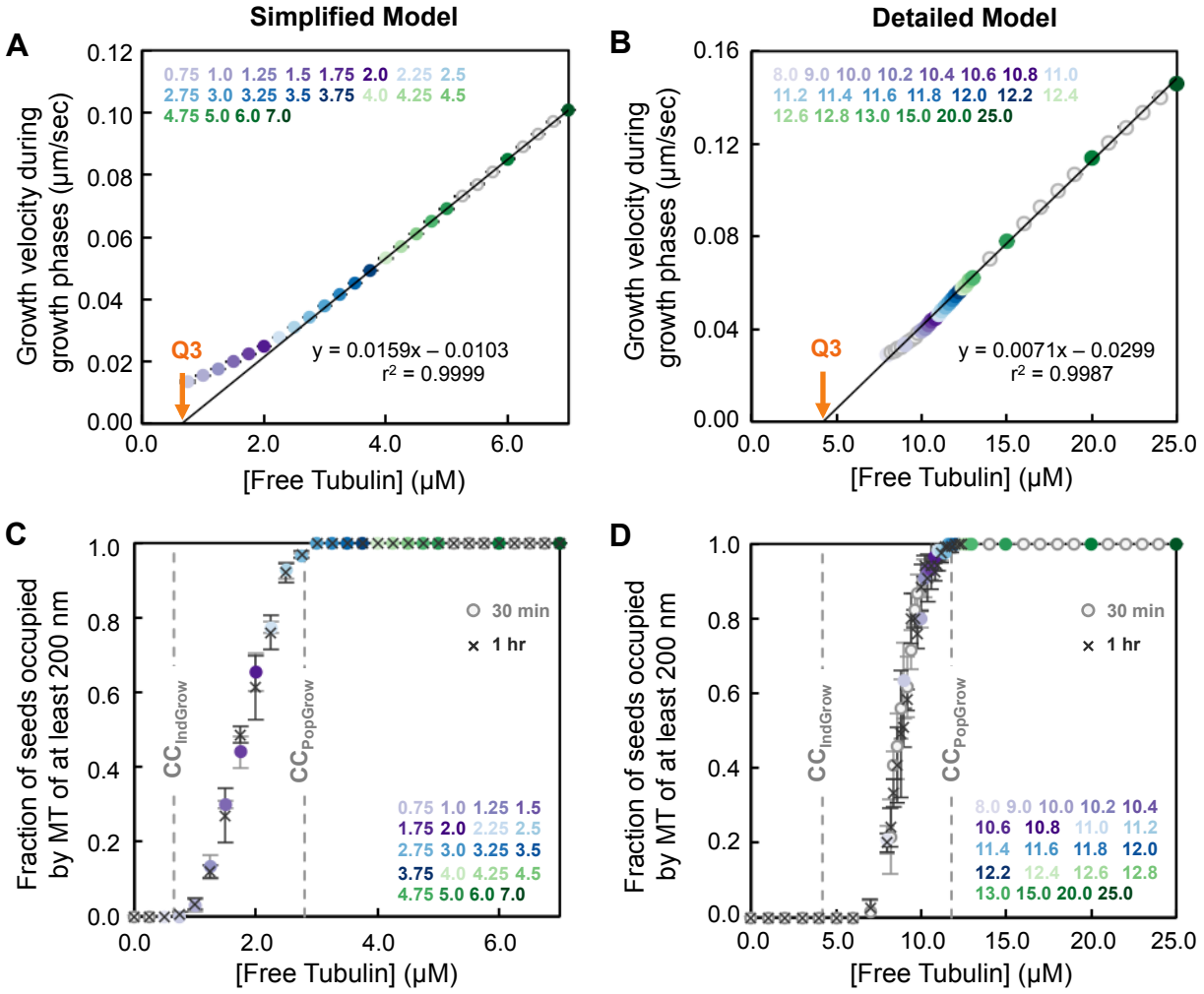
Simplified Model
Detailed Model
A
B
C
D
Growth velocity during growth phases (µm/sec)
[Free Tubulin] (µM)
Q3
y = 0.0159x – 0.0103
r² = 0.9999
y = 0.0071x – 0.0299
r² = 0.9987
Fraction of seeds occupied by MT of at least 200 nm
CC IndGrow
CC PopGrow
30 min
1 hr

Figure 6

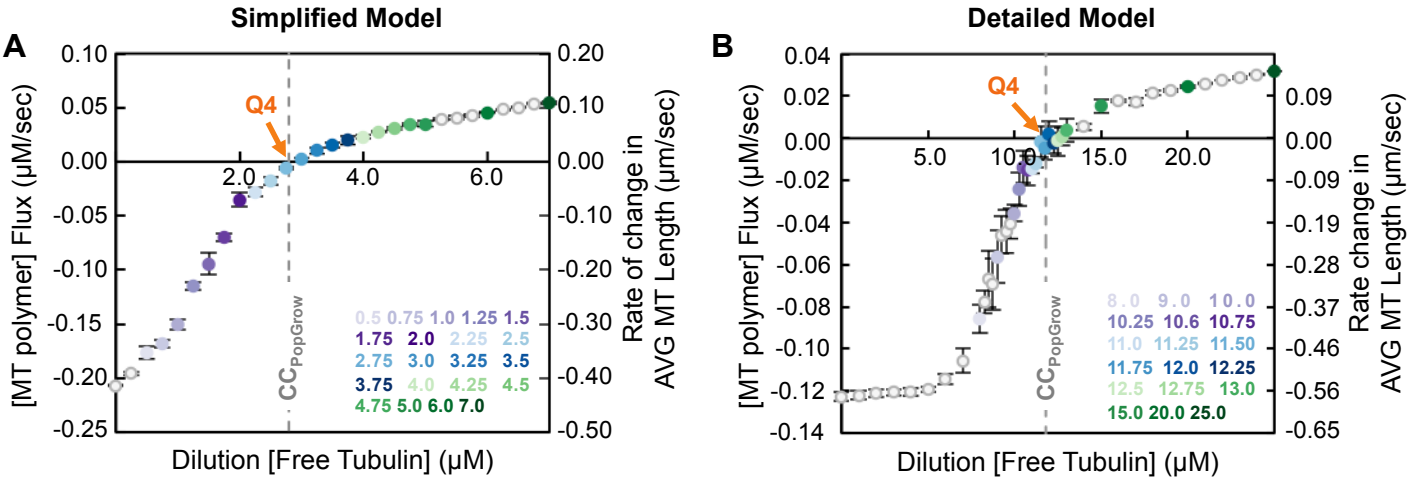
A
Simplified Model
Q4
CC PopGrow
[MT polymer] Flux (μM/sec)
Rate of change in AVG MT Length (μm/sec)
Dilution [Free Tubulin] (μM)
B
Detailed Model
Q4
CC PopGrow
[MT polymer] Flux (μM/sec)
Rate change in AVG MT Length (μm/sec)
Dilution [Free Tubulin] (μM)

Figure 7

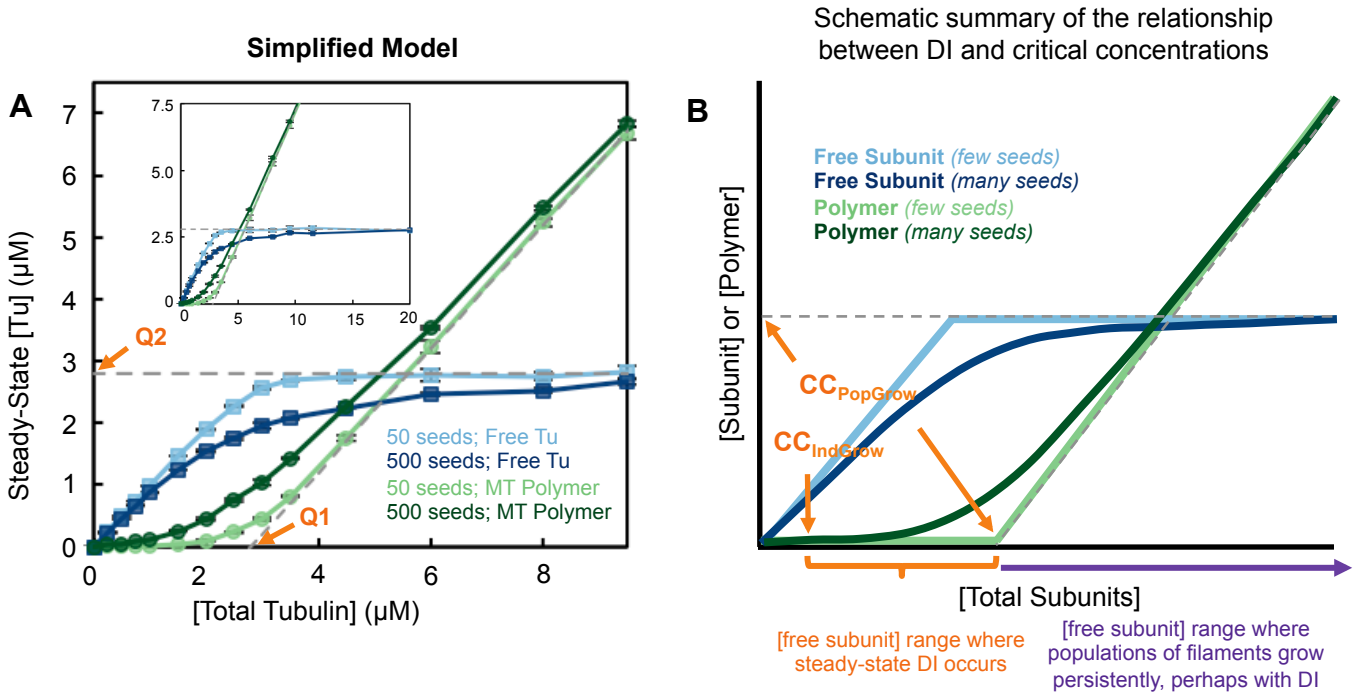
Simplified Model
A
Steady-State [Tu] (μM)
[Total Tubulin] (μM)
Q2
Q1
50 seeds; Free Tu
500 seeds; Free Tu
50 seeds; MT Polymer
500 seeds; MT Polymer
Schematic summary of the relationship between DI and critical concentrations
B
[Subunit] or [Polymer]
Free Subunit (few seeds)
Free Subunit (many seeds)
Polymer (few seeds)
Polymer (many seeds)
CC PopGrow
CC IndGrow
[Total Subunits]
[free subunit] range where steady-state DI occurs
[free subunit] range where populations of filaments grow persistently, perhaps with DI